Photocatalytic Water Oxidation Under Visible Light Irradiation By A Pyrochlore Oxide: Rhodium Substitution Into Yttrium Titanate

Borbala Kiss, Christophe Didier, Timothy Johnson, Troy D. Manning, Matthew S. Dyer, Alexander J. Cowan, John B. Claridge, James R. Darwent and Matthew J. Rosseinsky*

Abstract: A stable visible light-driven photocatalyst (≥ 450 nm) for water oxidation is reported. Rhodium substitution into the pyrochlore $Y_2Ti_2O_7$ is demonstrated through observation of Vegard's law evolution of the unit cell parameters with Rh content, to a maximum content of 3% dopant. Substitution renders the solid solutions visible light active. The overall rate of oxygen evolution is comparable to WO_3 but with superior light harvesting and surface area normalised turnover rates, making $Y_2Ti_{1.94}Rh_{0.06}O_7$ an excellent candidate for use in a Z-scheme water splitting system.

The photocatalytic splitting of water by visible light using semiconductor materials has been proposed as a route to sustainable hydrogen generation.[1] Of the systems available, Z-scheme photocatalysis offers several advantages over single particle photocatalysis or photoelectrocatalysis.[2] The Z-scheme system is inspired by natural photosynthesis in which two separate photocatalysts are linked by a shuttle redox mediator. In an artificial Z-scheme, each of the water splitting half-reactions is performed separately on each of the catalysts. Z-scheme systems lower the energy required for photocatalysis as the valence and conduction band edges of the individual photocatalysts do not have to straddle the reduction potentials of H^+/H_2 and O_2/H_2O as they do for a single particle photocatalyst. In this way a wider range of visible light can be used. Importantly using the Z-scheme approach, water splitting can take place in a simple reactor without the requirement for potentially costly electrode connections and transparent conducting supports. The production of oxygen is a critical step in solar fuels production and is a requirement for any photocatalytic water splitting system. This half of the water splitting process is more challenging since it typically involves a four-electron process and powerful oxidizing species which can lead to breakdown of the photocatalyst. It is also essential for photo-electrolysis. Whilst significant effort has been expended on developing visible light active hydrogen generating photocatalysts,[3] only a very limited number of stable, visible light active oxygen evolving photocatalysts are known.[4] Monoclinic WO_3 has been extensively studied as an oxygen generating photocatalyst and is generally used as the standard comparative material due to its commercial availability and reasonable performance.[5] However WO_3 has a relatively large band gap (2.6 eV) limiting its absorption of visible light to < 480 nm. Nanostructured $BiVO_4$ (E_g ~2.4 eV) [6] has been shown to photocatalytically generate oxygen under visible light irradiation and has a similar activity to WO_3.[7] Oxynitride perovskites have also displayed photocatalytic oxygen generation[8] but are less stable to photocorrosion than oxide materials unless OH^- is removed *in situ* by the addition of La_2O_3.[9] Recently Ag_3PO_4 has been demonstrated as a highly efficient oxygen evolving photocatalyst[10] though questions remain over its stability under reaction conditions.[11] Therefore to enable the development of an efficient Z-scheme for water splitting new stable, efficient, visible light active oxygen evolving photocatalysts are urgently required as highlighted in the recent review by Ma *et al.*[12]

The first reported photocatalyst for water splitting under ultraviolet (UV) radiation was TiO_2.[13] As a consequence, considerable attention has been given to titanium oxides, including the perovskite $SrTiO_3$ which also possesses photocatalytic activity for water splitting under UV irradiation.[14] Several substitutions for Ti have been evaluated in order to render these materials active under visible light,[15] with Rh reported as one of the most effective;[15b] $SrTi_{1-x}Rh_xO_3$ with Pt co-catalyst in an aqueous CH_3OH solution is a highly-active hydrogen evolving photocatalyst under visible light, and has been used with $BiVO_4$ or with WO_3 in a Z-scheme to split water with visible light.[16] Calculations[17] suggest that Rh E_g states are located within the conduction band in $SrTi_{1-x}Rh_xO_3$, allowing visible light excitation from the Rh T_{2g} to generate delocalized electrons which evolve hydrogen, however the formation of Rh^{4+} inter-gap states, that act as a recombination center for photoexcited carriers, can inhibit hydrogen evolution.

The $A_2B_2O_7$ pyrochlore structure (Figure 1a) consists of corner-sharing BO_6 octahedra with A cations in a 2+6 environment; there is one B-O-B angle which is around 135°.[18] The rare-earth $R_2Ti_2O_7$ pyrochlores thus have some structural similarities with perovskite $SrTiO_3$, which also features a corner-sharing TiO_6 octahedral network but with angles much closer to 180°. Pyrochlore is an important ternary oxide type which sustains a range of functions and is extensively tuneable by substitution.[18] Abe *et al*. have shown that pyrochlore $Y_2Ti_2O_7$ with NiO_x co-catalyst can be successfully used as a photocatalyst for water splitting under UV light, with a band gap of 3.5 eV.[19] As this gap is much larger than that of $SrTiO_3$, (3.2 eV), the Rh-derived E_g states in $Y_2Ti_{2-x}Rh_xO_7$ may sit just below the conduction band edge and thus become localised, potentially acting as recombination states or becoming photocatalytically inactive to hydrogen generation. The extensive chemical tuneability of pyrochlore suggests that suitable substitutions would enhance its photocatalytic properties and

[a] Miss B. Kiss, Dr. C. Didier, Mr. T. Johnson, Dr. T. D. Manning, Dr. M. S. Dyer, Dr. J. B. Claridge, Prof. J. R. Darwent, Prof. M. J. Rosseinsky
Department of Chemistry
University of Liverpool
Liverpool, L69 7ZD, UK
E-mail: M.J.Rosseinsky@liverpool.ac.uk
[b] Dr. A. J. Cowan
Stephenson Institute for Renewable Energy
University of Liverpool
Liverpool, L69 7ZF

Supporting information for this article is given via a link at the end of the document.

open up new directions in the synthesis of photocatalysts. This communication reports the phase-pure pyrochlore $Y_2Ti_{2-x}Rh_xO_7$ solid solution series and demonstrates its stable visible light activity as an oxygen evolving photocatalyst. Experiments in suspension establish this material as a promising candidate for inclusion in a Z-scheme, but we also note that $Y_2Ti_{2-x}Rh_xO_7$ is a potential photoanode.

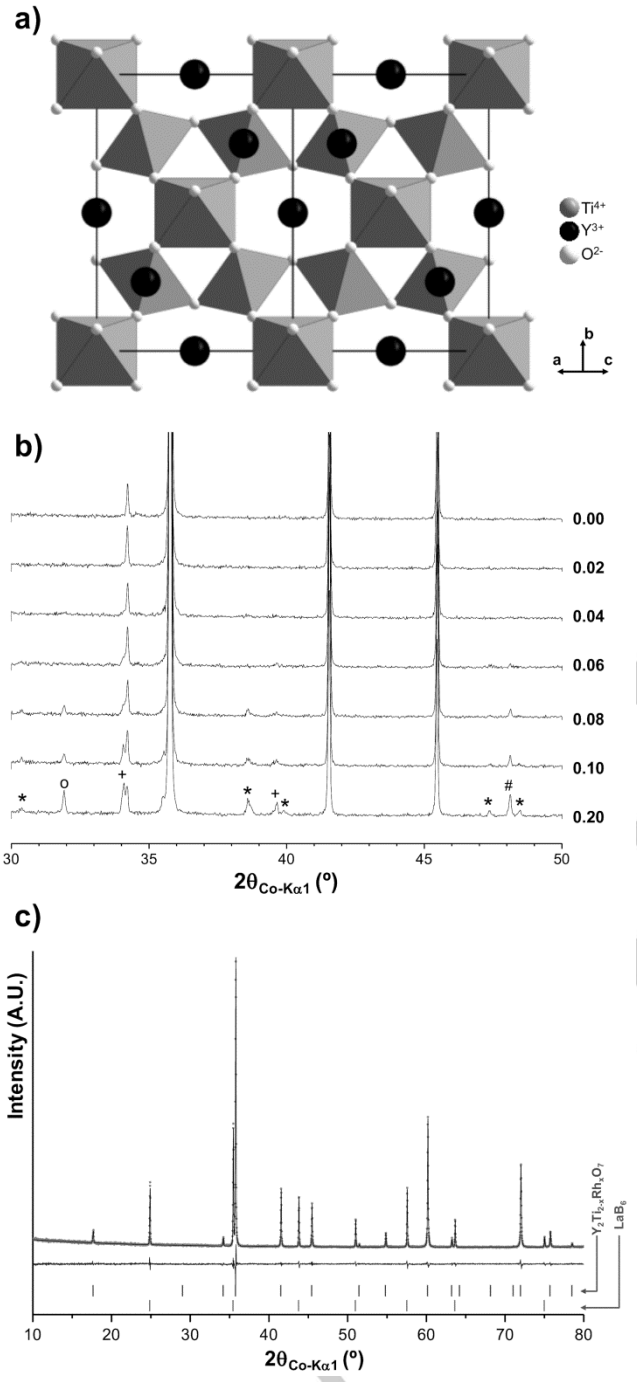

Figure 1. (a) Unit cell of the pyrochlore structure projected along the [101] direction, with the 6-coordinate Ti^{4+} sites represented by a network of grey corner-sharing octahedra, and Y^{3+} and O^{2-} ions represented by black and white spheres respectively. (b) Enlargement of the powder XRD patterns of $Y_2Ti_{2-x}Rh_xO_7$ with $0 \le x \le 0.2$ at the base of the peaks, showing impurities for $x > 0.06$. The main peaks ($x \ge 0$) denote the phase-pure cubic pyrochlore; impurities are indicated on the $x = 0.2$ doped sample: # Rh; o TiO_2; + Y_2O_3; * $YRhO_3$. (c) Le Bail whole pattern fitting of $Y_2Ti_{1.98}Rh_{0.02}O_7$, with LaB_6 as an internal standard.

The powder XRD patterns of the $Y_2Ti_{2-x}Rh_xO_7$ samples, prepared by solid-state synthesis, with $0 \le x \le 0.2$, are shown in Figure S1 and Figure 1b. All the samples contain a pyrochlore phase. However, as the comparison between Figure S1 and Figure 1b emphasizes, it is easy to miss crystalline impurities without a finer examination of the pattern. Non-pyrochlore peaks are observed for doping levels higher than $x = 0.06$, which have been assigned to Rh metal,[20] rutile TiO_2,[21] Y_2O_3[22] and perovskite $YRhO_3$.[23] The presence of metallic rhodium results from conversion of Rh_2O_3 to the metal at temperatures above 1100 ºC.[24] This suggests that $x = 0.06$ is the maximum amount of rhodium that can be inserted into the pyrochlore $Y_2Ti_2O_7$; however one cannot exclude the presence of impurities that are not visible from XRD. A superior proof of Rh substitution into the pyrochlore structure is the evolution of the unit cell dimensions upon substitution (Vegard's Law[25]).

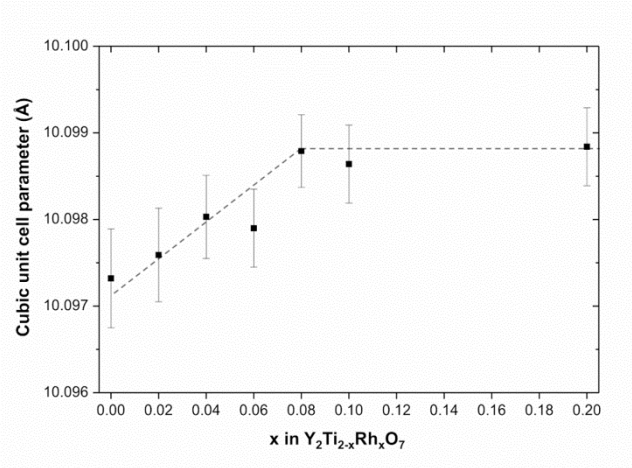

Figure 2. Unit cell parameter of $Y_2Ti_{2-x}Rh_xO_7$ determined from whole pattern fitting using the Le Bail method, using an LaB_6 internal standard. Error bars are 3 × e.s.d obtained from the refinement procedure, with Berar's factor included to ensure correlations are appropriately accounted for. Dashed lines are guides to the eye.

An internal standard was thus added in order to permit precise and accurate lattice parameter determination. The unit cell parameter of the pyrochlore $Y_2Ti_{2-x}Rh_xO_7$ were derived from whole pattern fitting using the Le Bail method. An example of the refinement profile is given in Figure 1c. The derived evolution of cell parameters with Rh concentration (Figure 2) is linear to $x = 0.08$, after which the unit cell parameter is constant. This behavior confirms the insertion of rhodium into the pyrochlore structure at these concentrations. Since the $x = 0.08$ sample was not phase-pure, $x = 0.06$ is the maximum amount of Rh that can be substituted into $Y_2Ti_2O_7$ under the synthetic conditions used here. The ionic radii of Rh^{4+} (0.615 Å[26] or 0.60 Å[27] though the latter is based on values from a number of metallic oxides) and Ti^{4+} (0.605 Å)[27] are very close, whilst that of Rh^{3+} (0.665 Å)[27] is significantly larger. The unit cell parameter changes observed are expected to be comparatively small in any solid solution

based on isovalent substitution, consistent with rhodium being present as Rh^{4+}. Substitution of Rh for Y is unlikely as the size difference between these cations is significant (1.019 Å for Y^{3+}),[27] and eight-fold or higher coordination for rhodium ions is very unusual. This substitution would also generate excess Y_2O_3 in the phase assemblage, which is not observed below the solubility limit (Figure 1). The possibility of substitution of Rh for Y in the $Y_2Ti_2O_7$ pyrochlore can thus be safely excluded.

The UV-visible absorption spectra, derived from the conversion of the diffuse reflection spectra, of $Y_2Ti_{2-x}Rh_xO_7$ ($0 \le x \le 0.06$) are shown in Figure 3a. The parent $Y_2Ti_2O_7$ has a measured indirect band gap of 3.71 eV (Figure S8) and does not absorb visible light.[19, 28] Substitution of Rh into $Y_2Ti_2O_7$ produces significant changes in the spectral response, with a red-shift of the absorption edge, together with the presence of two entirely new visible absorption features, giving light absorption down to 700 nm (Figure 3a, Figure S9).

Visible absorption peaks in Rh^{4+} substituted $SrTiO_3$ are associated with d-d transitions between Rh states just above the valence band and to a Rh inter-gap state and the conduction band.[15b, 17, 29] DFT calculations of the density of states (DOS) of $Y_2Ti_{1.75}Rh_{0.25}O_7$ (Figure 3b) reveal that, in addition to the inter-gap and near valence band states, Rh d-states are also manifest just below the conduction band of $Y_2Ti_2O_7$ upon Rh substitution. The computed DOS suggests that the lowest energy aborption feature (560 nm) results from a d-d transition from Rh d-states just above the valence band to the inter-gap state, and that the feature at 420 nm is a transition from the valence-band-edge to inter-gap state. The shift in absorption edge to lower energy cannot be attributed to a change in the fundamental O 2p – Ti 3d band gap, which remains almost unchanged in calculations. Rather a combination of transitions involving the localised Rh d-states just above the valence band, and those just below the conduction band have energies lower than the fundamental band gap, and effectively reduce the energy of the adsorption edge. On this basis the spectra have been fitted to two Gaussian peaks, an exponential function for the Urbach tail and a power-law dependant absorption edge (see ESI Section 8 for details) with a red-shift of the absorption edge to 3.12 eV for x = 0.06 and a tail that extends into the visible. The visible light activity of $Y_2Ti_{2-x}Rh_xO_7$ arises from one or more of the transitions arising due to the incorporation of Rh and leading to absorption in the visible region.

The $Y_2Ti_{2-x}Rh_xO_7$ series were investigated as photocatalysts for the evolution of H_2 and O_2 from water with visible light. No H_2 evolution was detected under visible light illumination using a 300 W Xenon lamp with 420 nm cut-off filter for any material, with or without co-catalyst. The materials did however display visible light activity for O_2 generation.

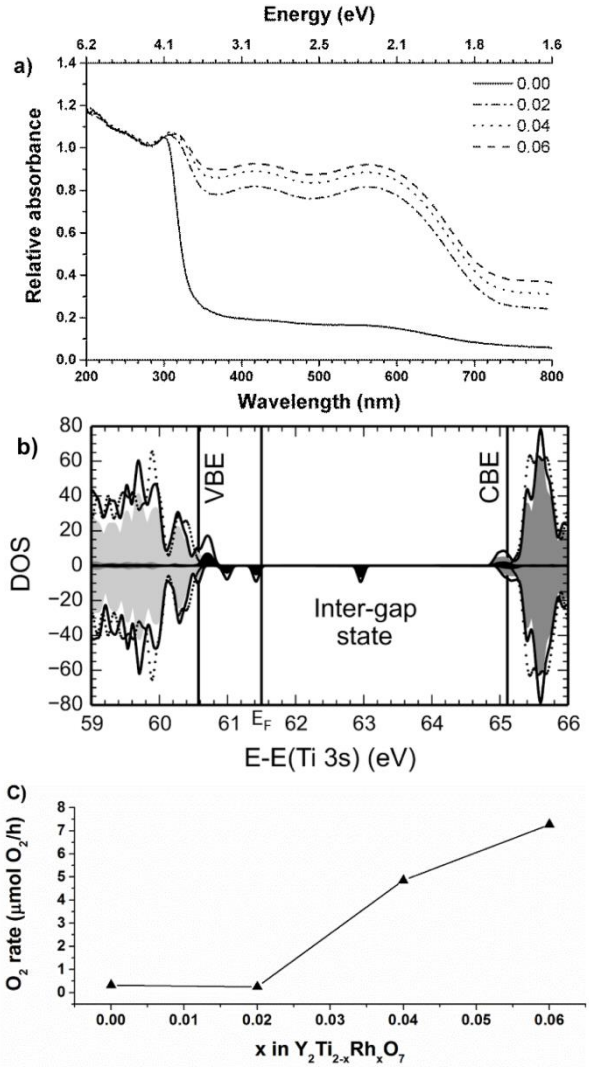

Figure 3. (a) UV-visible absorption derived from diffuse reflection spectra of $Y_2Ti_{2-x}Rh_xO_7$ ($0 \le x \le 0.06$); (b) The DOS of $Y_2Ti_2O_7$ (dotted line) and $Y_2Ti_{1.875}Rh_{0.125}O_7$ (solid line) are plotted along with the partial DOS projected onto the Ti 3d (mid-grey shaded), Rh 4d (black shaded) and O 2p (light grey shaded) orbitals of $Y_2Ti_{1.875}Rh_{0.125}O_7$ using the energy of the Ti 3s states as a common reference energy. The computed valence band edge (VBE) and conduction band edge (CBE) of $Y_2Ti_2O_7$ are indicated as vertical lines, along with the calculated Fermi energy of $Y_2Ti_{1.875}Rh_{0.125}O_7$ (c) Rate of O_2 generation using $Y_2Ti_{2-x}Rh_xO_7$ under visible light. 0.1 g of catalyst; no co-catalyst; 20 mL, 0.05 M $AgNO_3$(aq); 300 W Xe lamp (λ > 420 nm, <2.95 eV)

The O_2 evolution rate, measured with a Clark electrode,[5, 30] for unloaded $Y_2Ti_{2-x}Rh_xO_7$ ($0 \le x \le 0.06$) is represented in Figure 3c. The x = 0 and x = 0.02 materials did not show visible light activity. However, visible light photocatalytic O_2 evolution is observed for samples with $x \ge 0.04$. The activity increases up to $x > 0.06$ where it reaches a plateau $Y_2Ti_{1.94}Rh_{0.06}O_7$ displays excellent recyclability with no significant change in oxygen evolution rate over three cycles (Figure 4). The samples were examined by SEM and PXRD (Figure S2-S3) before and after the photocatalytic measurements and no indication of photocorrosion was observed. Oxygen evolution rates for both

WO_3, studied as a benchmark, and $Y_2Ti_{1.94}Rh_{0.06}O_7$ were confirmed by the widely used GC methodology using the same solution conditions as for the Clark electrode experiments and 400 ± 5 nm irradiation (Figure S4). Turnover rates per unit mass (TOR_m) and per unit surface area (TOR_s) have been suggested as useful comparisons between photocatalytic materials.[31] TOR_m for $Y_2Ti_{1.94}Rh_{0.06}O_7$ and WO_3 are similar (73 and 71 µmol/g/h respectively, Table S4). However there was a significant difference in TOR_s. The commercial WO_3 nanopowder has a BET surface area of 9.1 m^2/g giving TOR_s = 7.9 µmol/m^2/h; $Y_2Ti_{1.94}Rh_{0.06}O_7$ has a surface area of 3.2 m^2/g giving TOR_s = 22.8 µmol/m^2/h (Table S4). This suggests that increasing the surface area of $Y_2Ti_{1.94}Rh_{0.06}O_7$ by using alternative synthetic methods may further increase the photocatalytic activity of the material. For example sol-gel routes for $Y_2Ti_2O_7$ have been reported by several groups.[32] Apparent quantum efficiency values are given in Table S3: $Y_2Ti_{1.94}Rh_{0.06}O_7$ is superior to WO_3 at 450 nm and comparable at 400 nm at the illumination conditions used.

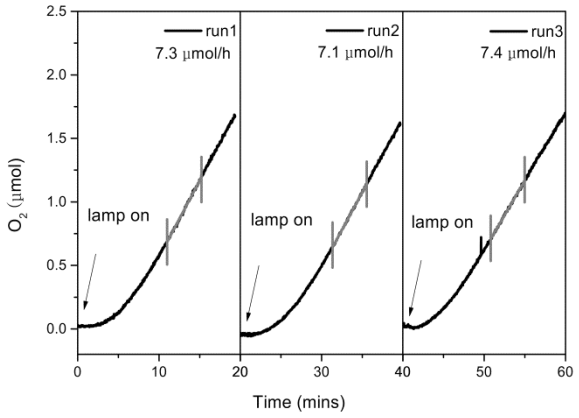

Figure 4. Recyclability of $Y_2Ti_{1.94}Rh_{0.06}O_7$ oxygen evolution photocatalyst; Catalyst, 0.1 g; no co-catalyst; 20 mL 0.05 M $AgNO_{3(aq)}$; light source, 300 W Xe lamp λ > 420 nm cut-off filter. The grey lines mark where the O_2 reaction rate was measured (µmol/min).

The addition of co-catalysts for water oxidation is a widely employed approach to enhance photocatalytic activity. In addition to the pure catalysts the effect of five of the most widely studied co-catalysts (Pt^0, Ru^0, NiO, RuO_2, $Rh_{2-y}Cr_yO_3$), identified to enhance the photocatalytic activity of other oxides for hydrogen and/or oxygen evolution, was investigated.[8] Protocols for co-catalyst loadings are provided in electronic supplementary information. Only the 1 % RuO_2 loaded $Y_2Ti_{1.94}Rh_{0.06}O_7$ showing a slight enhancement of the evolution rate (7.6 µmol/h) (Table S1, Figure S10-S11). Similarly an enhanced O_2 rate was reported for RuO_2/WO_3.[30a] Interestingly Ru metal loading (Figure S11) resulted in a large drop of the O_2 evolution activity. This inhibiting mechanism of Ru^0 in O_2 evolution has also been reported for Ru^0/WO_3.[30a] It is in fact not uncommon for co-catalyst to reduce activity for O_2 evolution.[33,34] Decreased photocatalytic activity in the presence of a co-catalyst is typically proposed to be due to increased electron-hole recombination losses, with either the co-catalysts themselves acting as recombination centres[33] or the deposition process leading to surface modifications and the formation of undefined recombination sites.

Advances in semiconductor materials for light-driven proton reduction to H_2 and for CO_2 reduction to carbon based fuels such as CH_3OH have led to an urgent requirement for improved, stable, visible light active water oxidation photocatalysts. Here we demonstrate that $Y_2Ti_{2-x}Rh_xO_7$ ($0.04 \le x \le 0.06$) is an efficient visible light photocatalyst for the generation of oxygen from water without the need for a co-catalyst. This opens the pyrochlore structure class for wider use as a photoelectrode and in Z-schemes for solar fuels production.

Acknowledgements

This work is funded by EPSRC (EP/H000925). AJC acknowledges the EPSRC for Fellowship EP/K006851/1. Computational resources were provided on ARCHER, through the UK's HPC Materials Chemistry Consortium, and funded by the EPSRC (EP/L000202). Dr R. Treharne is thanked for constructive conversations on the fitting of optical data

Keywords: pyrochlore • photocatalysis •titanates • water splitting

[1] a) The Hydrogen Economy: Opportunities, Costs, Barriers, and R&D Needs, The National Academies Press, **2004**; b) in Report of the Basic Energy Sciences Workshop on Hydrogen Production, Storage and Use, Argonne National Laboratory, **2004**.

[2] K. Maeda, *ACS Catal*. **2013**, 3, 1486-1503.

[3] F. Fresno, R. Portela, S. Suarez, J. M. Coronado, *J. Mater. Chem. A* **2014**, 2, 2863-2884.

[4] L. Yang, H. Zhou, T. Fan, D. Zhang, *Phys. Chem. Chem. Phys*. **2014**, 16, 6810-6826.

[5] W. Erbs, J. Desilvestro, E. Borgarello, M. Graetzel, *J. Phys. Chem*. **1984**, 88, 4001-4006.

[6] A. Walsh, Y. Yan, M. N. Huda, M. M. Al-Jassim, S.-H. Wei, *Chem. Mater*. **2009**, 21, 547-551.

[7] A. Kudo, K. Omori, H. Kato, *J. Am. Chem. Soc*. **1999**, 121, 11459-11467.

[8] T. Hisatomi, J. Kubota, K. Domen, *Chem. Soc. Rev.* **2014**, Advance Article (DOI: 10.1039/C3CS60378D).

[9] T. Takata, G. Hitoki, J. N. Kondo, M. Hara, H. Kobayashi, K. Domen, *Res. Chem. Intermed*. **2007**, 33, 13-25.

[10] a) Z. Yi, J. Ye, N. Kikugawa, T. Kako, S. Ouyang, H. Stuart-Williams, H. Yang, J. Cao, W. Luo, Z. Li, Y. Liu, R. L. Withers, *Nat. Mater*. **2010**, 9, 559-564; b) D. J. Martin, N. Umezawa, X. Chen, J. Ye, J. Tang, *Energy Environ. Sci*. **2013**, 6, 3380-3386.

[11] Y. Bi, S. Ouyang, J. Cao, J. Ye, *Phys. Chem. Chem. Phys*. **2011**, 13, 10071-10075.

[12] Y. Ma, X. Wang, Y. Jia, X. Chen, H. Han, C. Li, *Chem. Rev*. **2014** Advance Article (DOI: 10.1021/cr500008u).

[13] A. Fujishima, K. Honda, *Nature* **1972**, 238, 37-38.

[14] K. Domen, S. Naito, M. Soma, T. Onishi, K. Tamaru, *J. Chem. Soc. Chem. Commun*. **1980**, 543-544.

[15] a) H. Kato, A. Kudo, *J. Phys. Chem. B* **2002**, 106, 5029-5034; b) R. Konta, T. Ishii, H. Kato, A. Kudo, *J. Phys. Chem. B* **2004**, 108, 8992-8995; c) R. Niishiro, H. Kato, A. Kudo, *Phys. Chem. Chem. Phys*. **2005**, 7, 2241-2245; d) R. Asahi, T. Morikawa, T. Ohwaki, K. Aoki, Y. Taga, *Science* **2001**, 293, 269-271.

[16] Y. Sasaki, H. Nemoto, K. Saito, A. Kudo, *J. Phys. Chem. C* **2009**, 113, 17536-17542.

[17] S. Kawasaki, K. Akagi, K. Nakatsuji, S. Yamamoto, I. Matsuda, Y. Harada, J. Yoshinobu, F. Komori, R. Takahashi, M. Lippmaa, C. Sakai, H. Niwa, M. Oshima, K. Iwashina, A. Kudo, *J. Phys. Chem. C* **2012**, 116, 24445-24448.

[18] M. A. Subramanian, G. Aravamudan, G. V. Subba Rao, *Prog. Solid State Chem.* **1983**, 15, 55-143.

[19] R. Abe, M. Higashi, K. Sayama, Y. Abe, H. Sugihara, *J. Phys. Chem. B* **2006**, 110, 2219-2226.

[20] S. Fuyat, *Natl. Bur. Stand*. (U.S.), Circ. 539, **1953**, 3.

[21] F. Schossberger, *Z. Kristallogr., Kristallgeom., Kristallphys., Kristallchem*. **1942**, 104.

[22] Ľ. Smrčok, P. Ďuriš, in *X-Ray and Neutron Structure Analysis in Materials Science* (Ed.: J. Hašek), Springer US, **1989**, pp. 375-378.

[23] V. Lazarev, Shaplygin., *Russ. J. Inorg. Chem. (Engl. Transl.)* **1978**, 23, 1449.

[24] *CRC Handbook of Chemistry and Physics*, 80th Ed. ed., CRC Press, **1999-2000**.

[25] A. R. West, *Solid State Chemistry and its Applications*, 2 ed., Wiley, Hoboken, **2013**.

[26] R. D. Shannon, C. T. Prewitt, *Acta Crystallogr., Sect. B* **1969**, 25, 925-946.

[27] R. Shannon, *Acta Crystallogr., Sect. A: Cryst. Phys., Diffr., Theor. Gen. Crystallogr.* **1976**, 32, 751-767.

[28] B. V. Kumar, R. Velchuri, V. R. Devi, G. Prasad, B. Sreedhar, C. Bansal, M. Vithal, *J. Appl. Phys*. **2010**, 108, 044906.

[29] R. Niishiro, R. Konta, H. Kato, W.-J. Chun, K. Asakura, A. Kudo, J. *Phys. Chem. C* **2007**, 111, 17420-17426.

[30] a) J. R. Darwent, A. Mills, *J. Chem. Soc., Faraday Trans. 2* **1982**, 78, 359-367; b) Y. Zhang, J. Rosen, G. S. Hutchings, F. Jiao, *Catal Today* **2014**, 225, 171-176; c) N. M. Dimitrijevic, S. Li, M. Graetzel, *J. Am. Chem. Soc.* **1984**, 106, 6565-6569.

[31] I. E. Wachs, S. P. Phivilay, C. A. Roberts, *ACS Catal*. **2013**, 3, 2606-2611.

[32] a) O. Merka, D. W. Bahnemann, M. Wark, *ChemCatChem* **2012**, 4, 1819-1827; b) O. Merka, O. Raisch, F. Steinbach, D. W. Bahnemann, M. Wark, *J Am Ceram Soc*. **2013**, 96, 634-642; c) M. Higashi, R. Abe, K. Sayama, H. Sugihara, Y. Abe, *Chem. Lett*. **2005**, 34, 1122-1123.

[33] T. Sakata, K. Hashimoto, T. Kawai, *J. Phys. Chem*. **1984**, 88, 5214-5221.

[34] J. Yang, D. Wang, H. Han, C. Li, *Acc. Chem. Res*. **2013**, 46, 1900-1909.

Entry for the Table of Contents (Please choose one layout)

Layout 1:

COMMUNICATION

Visible-light activated water oxidation was achieved using rhodium substituted pyrochlore yttrium titanate, $Y_2Ti_{2-x}Rh_xO_7$ ($0 \le x \le 0.2$). A pure solid solution was obtained $x \le 0.06$, with visible light absorption to 700 nm. Compositions with $0.04 \le x \le 0.06$ showed stable oxygen generation without the need for co-catalyst loading.

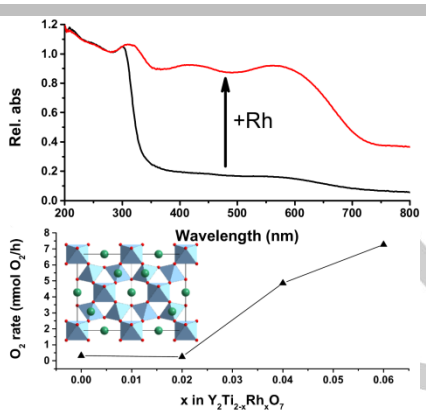

Borbala Kiss, Dr. Christophe Didier, Timothy Johnson, Dr. Troy D. Manning, Dr. Matthew S. Dyer, Dr. Alexander J. Cowan, Dr. John B. Claridge, Prof. James R. Darwent, Prof. Matthew J. Rosseinsky

Page No. – Page No.

Photocatalytic Water Oxidation Under Visible Light Irradiation By A Pyrochlore Oxide: Rhodium Substitution Into Yttrium Titanate